



## Corrosion inhibition of Cu-Ni (90/10) alloy in a medium (0.5M NaCl) by Nalco inhibitor of Diprochim

**Hamida Essom**

*Department of Metallurgy and Materials Engineering and, Laboratory LMGM, Faculty of Science of the engineer, Badji Mokhtar-Annaba University, PO Box 12, 23000 Annaba Algeria*

*Received 25 Jan 2015, Revised 12 May 2015, Accepted 12 May 2015*

\*Corresponding Author. E-mail: [Essom\\_h@yahoo.fr](mailto:Essom_h@yahoo.fr); Tel: (+216551708023)

### Abstract

The study relates to the characterization of the electrochemical behaviour of the alloy Cu-10Ni in the medium with 0,5M NaCl with and without inhibitor at the ambient temperature. The inhibiting effect of (NALCO based on amines) with various concentrations, was studied by the stationary and nonstationary electrochemical methods. The study thus underlined, a value of 35ppm, critical concentration in inhibitor at temperature 25°C, a rate of covering of the surface of 0,9243 for a maximum of effectiveness of 92,43%. Means of characterization such, cathodic and anodic polarization as well as optical microscopy and dispersive analysis X in energy (EDS), were used to characterize the external products of corrosion. A suitable equivalent land pattern was employed for calculates the various parameters. In agreement with the literature, the results of the curves of potentiodynamic polarization reveal that the inhibitor functions like an inhibitor mixed. Inhibition occurs by adsorption, creating a fall of the pH at the point of null load what returns the load of film of more negative surface with pH neutral and consequently less likely to the adsorption of species charged negatively like the ions Cl<sup>-</sup>. In comparison with the results, in agreement with the data of the literature [ ], the product of corrosion formed on alloy for a concentration of 35ppm in inhibitor, is a compound of CuO in the internal layer, and of CuO in the external layer. For a concentration higher than 35ppm, a porous and not-protective layer of corrosion is formed on alloy, its composition is a mixture of CuCl, Cu<sub>2</sub>O, NiO with traces of CuO and component most significant Ni(OH)<sub>2</sub>. The electrochemical spectroscopy of impedance (EIS) confirms the presence of an organic film external, playing the part of a barrier layer, protective side. The cyclic metric Volta diagrams obtained confirm the stability of protective film of the inhibitor even to the anodic potentials of +550 millivolts. All these studies indicate that the inhibitor reacts like an excellent inhibitor in the case of the alloy Cu-Nor 90/10) in the studied medium.

**Keywords:** 90Cu–10Ni alloys; B. EIS; B. Polarisation; B. OM; C. Passivity ; C. inhibitor efficiency

### 1. Introduction

Copper-nickel alloys are extensively used in marine applications and in desalination plants [2, 3] because of their good electrical and thermal conductivities, mechanical properties, corrosion resistance, and ease of fabrication of the equipment [1]. Several application principal are, the conduits of umpping of sea water, the tubes as condensers, sprays and exchangers of heat, in the water coolant circuits and of the medical services on board boats etc. Moreover, copper is well seen as a biodegradable metal in the environment following its potential to be 100% which can be recycled [1]. These systems should be regularly cleaned from carbonates and oxides that diminish their heating transmission. Diluted medium is used to clean these surfaces; a corrosion inhibitor is added to avoid the action of this medium on copper alloy. Amines and triazoles derivatives have been reported to be very effective inhibitors for copper in acidic solutions [2, 3]. The corrosion mechanism can vary considerably depending on the corrosive factors that are present. Similarly, the mechanism of inhibition will vary depending on the chemical nature of the inhibitor and the factor causing corrosion [4]. The most widely accepted postulated involves the formation of surface layers or films, which reduce the ease of access of the corrosive materials to the metal surface. Such scale can be formed naturally, or can be induced to form [5].

Many work reported that heterocyclic compounds, such as azoles, divulge marked effectiveness of [6-10]. This is why, organic inhibitors are largely used with success to protect copper and copper alloys against corrosion in different environments. [11-16]. These last year's several work was completed, on the problems of corrosion of the cupronickel tubes used in the units of distillation multi flash or MSF of desalination. The investigations try to describe the phenomena of corrosion of metals in various corrosive conditions with and without the presence of the inhibitor. The corrosion and impedance parameters, acting on the kinetics of corrosion behavior of Cu-Ni (90/10) alloy in seawater in the presence of at different concentrations of (NALCO) are evaluated and discussed.

## 2. Materials and methods

### 2.1. Experimental conditions

A traditional assembly with three electrodes includes an electrode of work, a platinum electrode and the reference electrode. The cell is connected to a potentiostat/galvanostat standard Gamry, controlled by computer coupled to a response recorder in frequency (FRA). The frequency range from 100000 kHz to 0,001 mHz under the excitation of sinusoidal wave of  $\pm 5$  mV amplitude. The potentiodynamic polarization studies were conducted in the potential range of  $-1,5$  V to  $+1.5$  V versus with a scan rate of  $1 \text{ mVs}^{-1}$ . The electrochemical and impedance studies were carried out at different concentrations, namely, 10, 20, 30, 35,40, and 60ppm.

### 2.2. Specimen preparation

The chemical compositions of Cu-Ni alloy were (0.148 %Sn, 1,43%Fe, 1,12%Zn, 0.015%Al, 0.0003%P, 0.5%Sb, 0.0583%Pb, 0.0202%Si, 0.017%S, 0.0056%As, 10%Ni, and the remainder is Cu). The cupronickel alloy specimens were taken from the same Cu-Ni (90/10) alloy sheet. For electrochemical studies, specimens with the dimensions of  $2.0 \times 2.0 \times 0.5$  cm were used by exposing  $0,786 \text{ cm}^2$  surface area, while the remaining area was insulated with epoxy resin. The exposed areas was mechanically abraded with various grade emery papers up to 1200 grades consecutively and were polished to mirror finish with alumina and water slurry on the micro polishing cloth. Then, these specimens were washed with triple distilled water, degreased with acetone before each experiment. The electrolyte used is a solution containing sodium chloride 0.5 M NaCl, with and without inhibitor. The electrolyte used was 100 ml for each experiment.

## 3. Results and discussion

### 3.1. Electrochemical impedance spectroscopy.

The impedance diagrams in Nyquist plot of Cu-Ni (90/10) alloy in 0,5M NaCl with and without of nalco inhibitor for different concentrations are presented in Figure 1. The Nyquist plots exhibit diffusion impedance at all the concentrations. The diameter of semicircular region increases with concentration of Inhibitor increase. This means that there is an increase in the charge transfer resistance ( $R_{ct}$ ). It can be noticed that the impedance modulus increased in presence of inhibitor. Though not clearly separated, these diagrams may be split into two capacitance loops. [17], The impedance spectra are then analysed with a non-linear regression calculation with a Simplex algorithm [18, 19], the calculation results are presented in Table 2. In this table,  $R_{sol}$  indicates the electrolyte resistance. The high frequency capacitance loop is attributed to the charge transfer resistance  $R_{ct}$  and the double layer capacitance  $C_{dl}$ . In presence of inhibitor,  $C_{dl}$  decreases, corresponding to the surface coverage by inhibitor observed by EDAX analysis. The low frequency capacitive loop  $C_F-R_F$  may be due to a faradic process involving the surface species issued of corrosion process and metallic species, such that  $M \leftrightarrow M^{2+} + 2e^-$ . The low frequency loop can be attributed to the Warburg impedance. The  $C_d$  values observed in absence and in presence of 35ppm Analco are those frequently reported for a flat electrode. In presence of 35ppm Analco, the value of  $C_d$  is markedly smaller corresponding to the adsorption of inhibitor or the film formation, but remains reasonable. The product of  $R_t$  by  $I_{corr}$  determined from polarisation curve in the reference solution is close to 20mV as often observed for the corrosion of metals at the active state, which validate the attribution of the first capacitance loop to the charge transfer resistance and the double layer capacitance. We will use EIS to evaluate further aspects of inhibiting efficiency of nalco. The value of  $C_F$  is compatible with the hypothesis on the origin of this loop attributed to an oxidation-reduction process involving corrosion products. In presence of nalco,  $R_F$  increases indicating that this compound stabilizes a species covering the electrode surface.

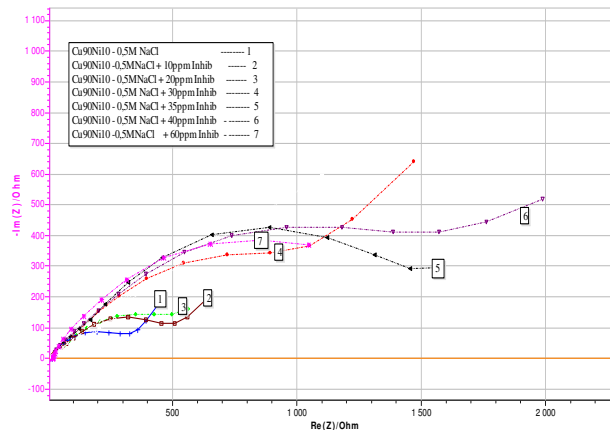


**Figure 1:** Nyquist (EIS) plots of Cu-Ni (90/10) alloy in Courbes of 0.5M NaCl with and without inhibitor.

The total impedance Bode plots, also indicates that the impedance increases with the concentration inhibitor increase figure 2. The phase angle Bode plots reveal that the phase maximum is the same at 35ppm and 60ppm and it shifts to a lower frequency at higher concentration. There is not only one maximum in all these plots and the angle corresponding to phase maximum is found to increase from 32° at 10ppm to 42° at 55° at 40ppm. All the above results infer that with the increase concentration inhibitor, the film is becoming more and more protective. In these Figures the  $|Z|$  ( $\Omega\text{cm}^2$ ) versus  $f$  (Hz) curves exhibit three distinctive segments. In the high frequency extreme region, the value of  $|Z|$  tends to become very small and the corresponding phase angle also falls of very rapidly with increasing frequency. This region is typical of a resistive behavior and corresponds to solution resistance. In the medium frequency region, a linear relationship exists between  $|Z|$  ( $\Omega\text{cm}^2$ ) and (Hz) and there is a broad maximum in the phase angle versus frequency plot.

**Table 1:** The impedance parameters

Parameters	concentration inhibitor						
	Blank	10ppm	20ppm	30ppm	35ppm	40ppm	60ppm
$R_{sol}$ ( $\Omega$ )	15,06	12,91	14,34	14,31	15,41	4,671	-
$R_{ct}$ ( $k\Omega.cm^2$ )	33,3	82,567	569,6	837,32	1037,12	467,13	-
$(CPE)_{dl}$ ( $\mu F.Cm^2$ )	13,32231	0,07322	0,05724	0,04252	0,03442	0,05284	-
$n_1$	0,6018	0,5676	0,6901	0,5554	0,743	0,5642	-
$R_{film}$ ( $k\Omega.Cm^2$ )	0,015	6,94	61,18	187,6	249,1	175,2	-
$(CPE)_{film}$ ( $\mu F.Cm^2$ )	16,13	0,37223	0,1823	$-83,5 e^{-3}$	0,06300	0,05104	-
$n_2$	0,5616	0,58	0,648061	0,7285	0,84001	0,718979	-
Warburg	-	15,81	126,2	66,88	45,74	-	-
$\Sigma\chi^2$	0,004439	0,079	0,001976	0,004822	0,00445	0,061	-
IE%	-	59,66	94,15	<b>96,02</b>	96,78	92,87	-

This region corresponds to the charge transfer at the metal/electrical double layer. In the low frequency segment, the resistive behavior of the electrode increases and the value of  $|Z|$  ( $\Omega\text{cm}^2$ ) should remain constant with a further decrease in frequency. But such behavior is not found  $|Z|$  ( $\Omega\text{cm}^2$ ) still increases, with a decrease in frequency. This corresponds to the diffusion impedance because of the diffusion of oxygen and chloride

from the bulk of the solution to the interface at the instant of the immersion of the electrode in electrolyte and also of  $\text{CuCl}_2^{2-}$  species from the interface into the bulk of the solution at higher concentration of inhibitor, besides diffusion of oxygen and chloride from solution to the interface [20]. In order to account for the above results, the metal/solution interface is modeled as per the equivalent circuit shown in Figure 3 [21] and the best fit is obtained for the experimental results with this model. In this model constant phase element (CPE) is substituted for the double layer capacitance to give a more accurate fit [22 -25]. The values of the elements in the equivalent circuits described in Fig. 3. It is clear that the charge transfer resistance,  $R_{ct}$  of the alloy is increasing from concentration 10ppm to 35ppm, indicating that corrosion rate decreases with concentration of inhibitor. However, it is interesting to note that the increasing rate of  $R_{ct}$  gradually decreases with concentration of inhibitor beyond 35ppm. During the initial exposure, the  $R_{ct}$  increases after 10ppm from 33,3 to 82,56 k $\Omega$ ; whereas it increases sharply from 569,61 k $\Omega$  from 1037,12 for 25ppm. This is caused by the growth of the passive oxide film on the alloy surface. As shown in Table 1, the change in the resistance of the passive oxide film,  $R_f$ , with concentrations of inhibitor is more complicated. The  $R_f$  is about 6,94 k $\Omega$  after 10ppm of inhibitor, indicating the formation of a thin, protective and compact oxide film. Radford et al. [26] reported that a layer of protective oxide film can be formed on the surface of the 70/30 Cu–Ni alloy within a very short time. It is valuable to point out that the outer porous and non-protective oxide film seems to appear with 10ppm of inhibitor; and it gradually becomes thicker with time. At the same time, the inner protective compact oxide film also grows in thickness.

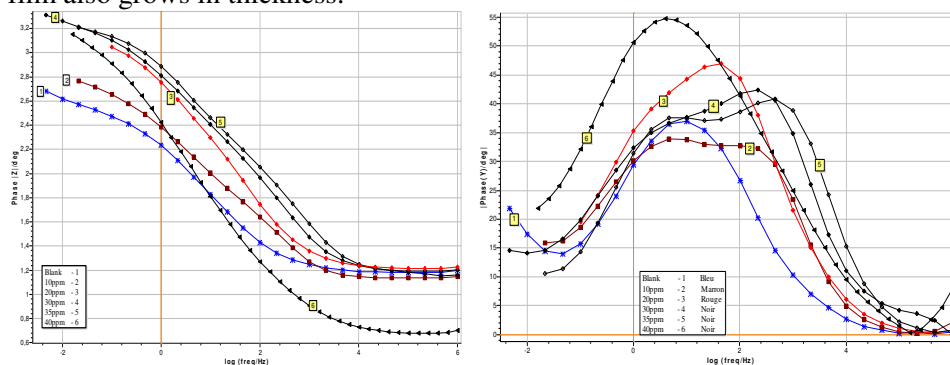


**Figure 2.** Bode plots of Cu-Ni (90/10) alloy in medium 0.5M NaCl with and without inhibitor.

The increases in  $R_{ct}$  and  $R_{film}$  with inhibitor shown in Table 1 confirm this point. After 35ppm, the resistance of the outer oxide film is 249,1 k $\Omega$  ; while the resistance of the inner oxide film is up to 1037,12 k $\Omega$  . In addition, the values of  $n_2$  of the outer oxide film are stabilized with the increase in the concentration of the inhibitor, possibly indicating an increase in surface heterogeneities on the surface.

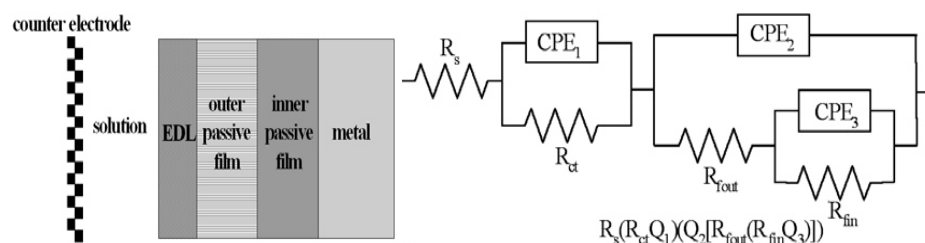


**Figure 3.** Equivalent circuits modeling the electrode used to calculate the impedance parameters

In light of these results, it is easy to conclude that a multilayer oxide film is formed on the surface when exposed to medium with inhibitor 35ppm, and that the inner layer of the oxide film is mainly responsible for the good corrosion resistance, and the film is composed of  $\text{Cu}_2\text{O}$  doped with nickel or trace addition element. The Bode plots figure 2 are quite interesting. The phase angle Bode plots show that there is a shift of frequency corresponding to phase maximum from about 5 Hz in the absence of Analco to a much higher frequency in the presence of 20ppm of Analco. The angle corresponding to phase maximum is also increased from 16° to about 47°. A close examination of these plots reveals that there is a possibility of two time constants. It is interesting

to note that with a further increase in the concentration of the inhibitor to 35ppm, there is a shift in the phase maximum to a lower frequency side and phase angle is increased to about 55°. The total impedance is increased to a very great extent in the presence of the inhibitor and with the increase in the concentration of the inhibitor. There is more broadening of the phase maximum with the increase in the concentration of the inhibitor. This result reveals that the protective nature of the inhibitor film is increased with the increase in the concentration of the inhibitor. The electrochemical system may be modeled as consisting of metal/protective surface film/electrical double layer/electrolyte solution. Therefore, for all the systems, in the presence of Analco, the equivalent circuit is used. The experimental data fitted with this equivalent circuit better than with other equivalent circuits reported in the literature [27- 29]. The corresponding impedance parameters are given in Table 1. It is interesting to note that both  $R_{ct}$  and  $R_{film}$  are increased with the increase in the concentration of the inhibitor. An increase in  $R_{ct}$  from 33,3 to 1037,12  $k\Omega\ cm^2$  and an increase in  $R_{film}$  from 0.015 to 249.1  $k\Omega\ cm^2$  are obtained by the addition of 35ppm of Analco to medium 0,5M NaCl. An IE% of 96.78 is obtained at 35ppm concentration of Nalco.

**Table 2.** Effect of Analco on the electrochemical kinetics of Cu–10Ni in 0,5M NaCl with or without inhibitor. Electrochemical parameters and effectiveness (10-60)ppm.

	Milieu 0,5 M NaCl with concentration d'Inhibiteur (nalco)					
	Ecorr mV	Icorr $\mu$ A	$\beta_a^b$ $\mu$ V/decade	$\beta_c^a$ $\mu$ V/decade	Cor Rate mmpy	$\eta$ %
Blanc	-716,547	37,517	-	333,0	0,58	-
10 ppm	-318,9	5,66	90,7	205,5	0,087	84,91
20ppm	-296,21	4,64	89,6	196,5	0,071	87,63
30 ppm	-306,44	4,21	95,2	167,1	0,065	88,77
35 ppm	-307,38	2,78	75,4	158,7	0,058	<b>92,592</b>
40 ppm	-299,0	12,54	91,6	315,5	0,194	66,57
60ppm	-257,40	13,23	71,25	411,0	0,304	62,73

<sup>a</sup>  $\beta_c$  is the Tafel slope of cathodic polarization curve.

<sup>b</sup>  $\beta_a$  is the Tafel slope of anodic polarization curve.

Both the  $(CPE)_{dl}$  and  $(CPE)_{film}$  values are reduced to extremely small values of 0.034 and 0.051  $\mu F\ cm^{-2}$ , respectively, in the presence of nalco and the corresponding “n” values are increased to 0.74 and 0.84, respectively. These results reveal that the concentration of nalco molecules in the protective film is increased and the  $Cu_2O$  formation is much less. Nalco molecules replaced almost all the water molecules and the ions in the electrical double layer. As a protective film with a high charge transfer resistance is formed when the concentration of nalco is 35ppm. The corresponding Nyquist and Bode plots are shown in Figures (1) and (2), respectively. The impedance parameters are given in Table 2.

### 3.2. Potentiodynamic Polarization Studies.

Each experiment was carried out with a freshly abraded electrode. The electrode was first left at the open-circuit conditions during 30 min. Then, the anodic and cathodic polarization curves were recorded. The potentiodynamic polarization curves for Cu-Ni (90/10) alloy in 0,5M NaCl at different concentrations of nalco at 02h immersion, (Temperature:30°C) in the potential range from -1.5 to +1.5 V are given in figure 4. The anodic polarization curves show three distinct regions, namely, Tafel region at lower over potentials extending to the peak current density due to the dissolution of copper to  $Cu^+$  ions [30], a region of decreasing current density until a minimum ( $i_{min}$ ) is reached due to the formation of  $CuCl$ , and a region of the sudden increase in current density leading to a limiting value ( $i_{lim}$ ), due to the formation of  $CuCl_2^-$  [31]. With the increase in concentration of nalco, the corrosion potential ( $E_{corr}$ ) is shifted towards more positive value and the shift in cathodic Tafel slope ( $\beta_c$ ) is greater than the shift in anodic slope ( $\beta_a$ ).

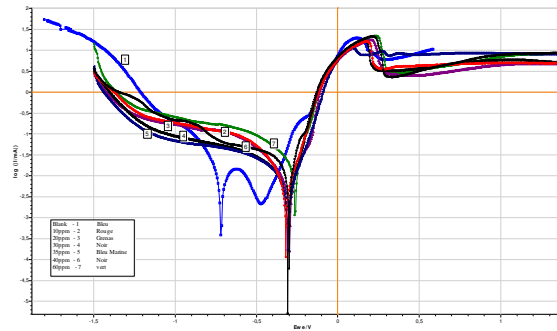


**Figure 4:** The polarization curves.

However, the corrosion current density ( $i_{corr}$ ) is found to decrease significantly up to 30ppm and then increase slightly up to 35ppm. These results infer that with the increase concentrations up to 35ppm, there is a decrease in the corrosion rate of the alloy due to the formation of copper oxide film inhibited, and this has been reported by many investigators [32-34]. Another interesting feature is that while there is only one anodic peak for 10 and 20ppm, there are two anodic peaks after 30 and 35 ppm at 100 - 150 and 250 - 300 mV, respectively Figure 5 a), b), c). The larger peak at 100-150 mV is due to the oxidation of Cu to  $Cu^+$  ions and the smaller peak at 250 - 300 mV is due to the oxidation of  $Cu^+$  to  $Cu^{2+}$  ions.

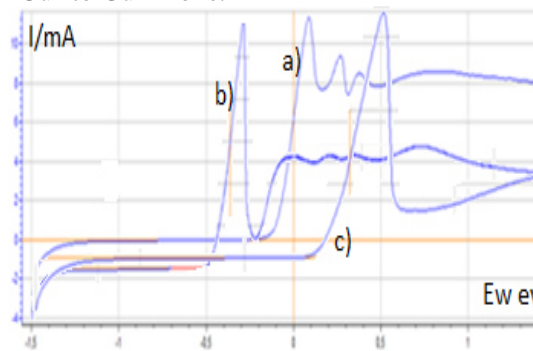


**Figure 5:** a), b), c), anodic curves of Cu-Ni (90/10) alloy in 0,5M NaCl

The current peak observed at 0.1- 0.4V in absence of Analco figure 5a disappears progressively by increasing the inhibitor concentration. For an Analco concentration higher than 35ppm, no current peak is observed. The current increases for higher potentials by the passive film breakdown.



**Figure 6.** Optic picture of Cu–10Ni surface in 0,5M NaCl without 35 ppm of nalco (a) and (b) with 35 ppm.

### 3. 3 Cyclic Voltammometric Studies.

The cyclic voltammograms of Cu-Ni (90/10) alloy in the potential range from  $-1.0$  to  $+1.0$  V. After 1- and 8-hour immersion periods are given in Figures 8(c) and 8(d), respectively.

At both immersion periods, in the first cycle, in the forward sweep, they show two anodic peaks. The first peak at  $+250$  mV is due to ( $Cu - Cu^+$ ) couple and the second one at  $+450$  mV is due to ( $Cu^+ - Cu^{2+}$ ) couple.

Two corresponding reduction peaks are observed in the reverse sweep. In the second cycle also the same behavior is seen. Both the anodic and cathodic peak current densities are increased to some extent in the second

cycle. In the presence of 35ppm after 1-hour immersion period (Figure 8(a)), in the first cycle there is no anodic peak up to +500 mV. With the increase in immersion period up to 8 h (Figure 8(b)), the film became more protective even up to +550 mV.

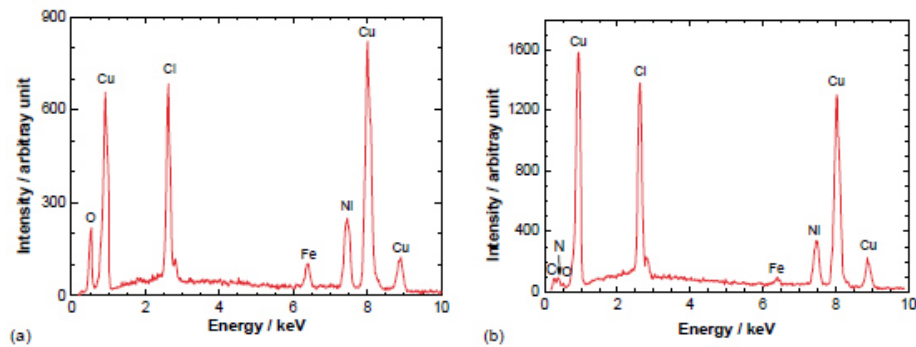


**Figure 7.** EDAX spectra obtained at the alloy surface after 02 h immersion in 0,5M NaCl test solution (a) without and (b) with of nalco.

In the second cycle, similar behavior of bare alloy in the absence of NALCO is seen because of the breakdown of the film as a consequence of the application of higher potentials up to 1.0 V. The  $C_V$  profiles confirm that inhibitor functions excellently and protects the Cu-Ni (90/10) alloy from corrosion in a medium 0,5NaCl.

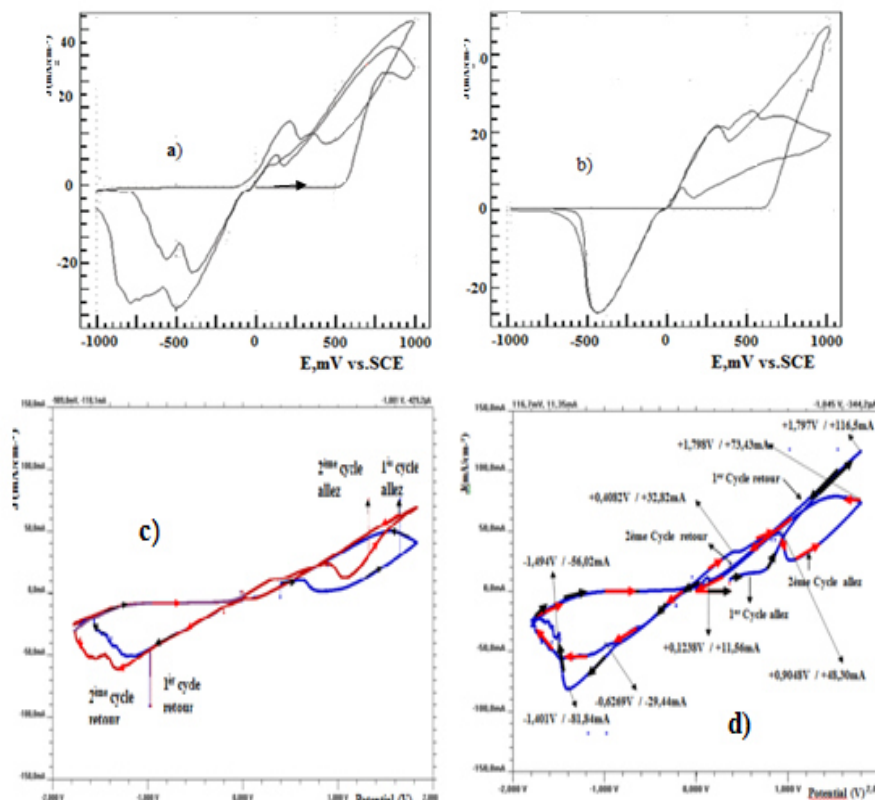


**Figure 8.** Cyclic voltammograms of copper- nickel (90/10) alloy in medium 0,5M NaCl with of 35ppm nalco (a) 1h,( b) 8h and without of 35ppm nalco (c) 1h,( d) 8h ( Temperature 25°C).

### 3.4 Surface film formed upon Cu-10Ni surface by corrosion

Fig. 6 presents the surface morphology in the presence of 35ppm concentration of nalco in medium 0.5M NaCl solution. In contrast, in presence of nalco (Fig. 6b), almost no corrosion is revealed, and the grooves due to the initial surface abrasion remain clearly visible after 8 h immersion. Some precipitates observed are NaCl crystals appeared, because of insufficient surface rinsing. The comparison of these two figures reveals a marked inhibiting efficiency of Nalco.

## Conclusion

Electrochemical study showed that nalco product tested is a good corrosion inhibitor, against Cu–10Ni corrosion in medium of 0,5M NaCl at pH 7.25. The inhibitor acts at the same time on the anodic and cathodic electrochemical processes. Polarisation curves showed that the inhibiting effect of this compound results in a clear reduction of the cathodic and anodic current density values especially in the vicinity of corrosion potential. Potentiodynamic polarization studies indicated that nalco considerably shifts the corrosion potential to less negative values and greatly decreases the corrosion current density. A remarkable inhibiting effect of nalco was observed when its concentration is higher than 35 ppm. These results were confirmed by impedance tests where it was observed that the effect of inhibitor addition is distinguished by an increase of the resistance and a strong reduction of the electrochemical interface capacity value. Inhibition efficiency of this compound depends on its concentration. Indeed, it increases as the concentration of inhibitor increases until 35ppm. The protective effect improves with increase of immersion period, and reached values as high as 92,43%. for 35ppm of concentration. Addition of inhibitor modifies the characteristics of the interface Cu–130Ni / 0,5M NaCl pH 7.25. All the three electrochemical methods reveal that nalco is proved to be an excellent inhibitor for Cu-Ni (90/10) alloy in medium 0,5M NaCl with 35ppm. Surface examination studies by EDX confirm the presence of protective film on the alloy surface. This inhibitor may be applied in coolant circuits using sea water like cooling fluid.

## References

1. John Wiley & Sons., *Uhlig's Corrosion Handbook, Second Edition, Edited by R. Winston Revie*, ISBN 0-471-15777-5, (2000), , Inc. p.729.
2. Sherif M., Erasmus M., and Comins D., *J. Colloid, Interface Sci*, 311 (2007) 144.
3. Sherif M., Park S., *J. Electrochim Acta*, 51 (2006) 4665.
4. Fiala A., Chibani A., Darchen A., Boulkamh, and Djebbar K., *Appl. Surf. Sci.*, 253 (2007) 9347.
5. Trachli B., Keddam M., Srhiri A., Takenouti H., *Corros. Sci*, 44 (2002) 997.
6. Otmac'ic H., Stupniš'ek-Lisac E., *Electrochim. Acta*, 48 (2003) 985.
7. El Issami S., Bazzi L., Hilali M., Saloghi R., Kertit S., *Ann. Chim. Sci. Mat*, 27 (2002) 63.
8. Dafali A., Hammouti B., Makhliše R., Kertit S., *Corros. Sci*, 45 (2003) 1619.
9. Huynh N., Bottle S.E., Notoya T., Trueman A., Hinton B., Schweinsberg D.P., *Corros. Sci*, 44 (2002) 1257.
10. Wang L., *Corros. Sci*, 43 (2001) 2281.
11. A. Al-Hachemi, J. Carew., *Desalination*, 150 (2002) 255.
12. Spah M., Spah D. C., Deshwal B., Lee S., Chae Y-K., Park J. W., *Corros. Sci*, 51 (2009)1293.
13. Badawy W. A., Ismail K. M., and Fathi A. M., *Electrochimica Acta*, 51 (20) (2006) 4182.
14. Benmessaoud M., Es-salah K., Hajjaji N., Takenouti H., Srhiri A., and Ebn Touhami M., *Corrosion Science*, 49 (10) (2007) 3880.
15. Allam N. K., Ashour E. A., Hegazy H. S., El-Anadoulı B. E., and Ateya B. G., *Corrosion Science*, 47 (9) (2005) 2280.
16. Trachli B., Thesis, P&M Curie University–Kenitra University, November, 2001.
17. Gennero M.R., De Chialvo, S.L. Marchiano, A.J. Arvia., *J. Appl. Electrochem*, 14 (1984) 165.
18. Kato C., Ateya B.G., Castle J.E., Pickering H.W., *J. Electrochem. Soc*, 127 (1980) 1890.
19. Wood R.J.K., Hutton S.P., Schiffrin D.J., *Corros. Sci*, 30 (1990) 1177.
20. Kear G., Barker B.D., Stokes K., Walsh F.C., *J. Appl. Electrochem*, 34 (2004) 659.
21. Tait W.S., *An Introduction to Electrochemical Corrosion Testing for Practicing Engineers and Scientists*, University of Wisconsin-Madison, Racine, USA, (1994).
22. Boukamp B.A., *Equivalent Circuit Users Manual*, second ed., *University of Twente*, Netherlands, (1993).
23. Zhang X.H., Pehkonen S.O., Kocherginsky N., Ellis G.A., *Corros. Sci*, 44 (2002) 2507.
24. Radford G.J.W., Walsh F.C., Smith J.R., Tuck C.D.S., Campbell S.A., *Developments in Marine Corrosion*, *Royal Society of Chemistry*, Cambridge, (1998) 41.
25. Badawy W. A., Ismail K. M., and Fathi A. M., *Journal of Applied Electrochemistry*, 35 (9) (2005) 879.
26. Badawy W. A., Ismail K. M., and Fathi A. M., *Electrochimica Acta*, 51 (20) (2006) 4182.
27. Yuan S. J. and Pehkonen S. O., *Corrosion Science*, 49 (3) (2007) 1276.
28. Sherif E. M., Erasmus R. M., and Collins J. D., *Journal of Applied Electrochemistry*, 39 (1) (2009) 83.
29. Alfantazi A. M., Ahmed T. M., and Tromans D., *Materials and Design*, 30 (7) (2009) 2425.
30. Kato C., Ateya B. G., Castle J. E., and Pickering H. W., *Journal of the Electrochemical Society*, 127 (9) (1980) 1890.
31. Wang Y. Z., Beccaria A. M., and Poggi G., *Corrosion Science*, 36 (8) (1994) 1277.
32. Popplewell J. M., Hart R. J., and Ford J. A., *Corrosion Science*, 13 (4) (1973) 295.